5-2011

TRPM4/5's Role in Inspiratory Calcium-Activated Nonspecific Cation Current

Adam Mitchell Goodreau
College of William and Mary

TRPM4/5's Role in Inspiratory Calcium-Activated Nonspecific Cation Current

A thesis submitted in partial fulfillment of the requirement
for the degree of Bachelor of Science in Biology from
The College of William and Mary

by

Adam Mitchell Goodreau

Accepted for _____

_____

Margaret S. Saha, Director

_____

Mark H. Forsyth

_____

Diane C. Shakes

_____

Gregory D. Smith

Williamsburg, VA
May 5, 2011

Contents

Preface

Acknowledgements

This work was funded by grants in support of undergraduate research from the Howard Hughes Medical Institute Undergraduate Science Education Grant awarded to The College of William and Mary (M.S. Saha, Project director).

I would like to thank Professor Christopher A. Del Negro of the Applied Science department for years of guidance and support as well as his continued patience in advising me from France. I would also like to thank Professor Saha for serving as the director of my thesis committee during Professor Del Negro's sabbatical, as well as Professors Forsyth and Shakes of the Biology department and Professor Smith of the Applied Science department for serving on my committee and offering their respective expertise in evaluating this work.

Additionally, I extend thanks to our colleagues and collaborators at other institutions: Romain Guinamard of the Groupe Coeur et Ischémie, Université de Caen in Caen, France for his guidance in troubleshooting our single-channel protocols and Ryoichi Teruyama at Lousiana State University for his immunohistochemistry work. Finally, I would like to thank my undergraduate colleague, Thomas B. Arnold, for his contributions to this project and for continuing this investigation in the year to come.

Abstract

In mammals, the breathing behavior originates in brainstem networks. Neurons of the mammalian respiratory rhythmogenerator, the preBötzinger complex (preBötC), augment periodic synaptic input to generate robust envelopes of depolarization called *inspiratory drive potentials*. Calcium-activated non-specific cationic current (I_{CAN}) has been implicated in drive potential generation via an inositol 1,4,5-trisphosphate (IP_3) dependent mechanism. The protein or proteins underlying this current, however, remain unknown. Because of their unique biophysical properties, two homologs of the transient receptor potential (TRP) channel family, TRPM4/5, make attractive candidates for (I_{CAN}). Earlier RT-PCR experiments demonstrated expression of TRPM4/5 mRNAs within the preBötC. Additionally, using anatomical landmarks, earlier immunohistochemical data demonstrate expression of TRPM4/5 protein in neurons of the inspiratory network. Here, we provide the first functional evidence for TRPM4/5 in the preBötC. Pharmacological inhibition of TRPM4 by a selective inhibitor, 9-phenanthrol, progressively attenuated drive potentials, consistent with a functional role for TRPM4 in inspiratory burst generation. Additionally, we propose a protocol that will facillitate single-channel recordings from preBötC neurons. We conclude that, while not definitive, many lines of evidence now suggest TRPM4/5 channels as the molecular identity of I_{CAN}.

Chapter 1

Introduction

1.1 The Neural Control of Breathing

In mammals, the breathing behavior is biphasic: an active phase draws air into the lungs and a passive phase forces it out. The active phase, called inspiration, is characterized by rhythmic contractions of the diaphragm and external intercostal muscles that increase the superior-inferior space of the thoracic cavity, lowering the intrapulmonary pressure (P_{pul}) (Marieb, 2009). A pressure gradient develops such that atmospheric pressure (P_{atm}) is greater than intrapulmonary pressure ($P_{\text{atm}} > P_{\text{pul}}$) and air is drawn into the thoracic cavity. Passive expiration occurs as the inspiratory muscles relax, decreasing the volume of the thoracic cavity, reversing the pressure gradient, and expelling air from the lungs. Oscillations between these respiratory phases provide tissues oxygen needed for metabolism while removing gaseous metabolic waste. This behavior begins at birth, persists until death, and remains adaptable to the organism's development, activity, and environment (Feldman and Negro, 2006).

The movements of breathing are rhythmic and, in healthy mammals, in healthy mammals, simple. However, this behavior is the product of an elaborate neural network in the lower brainstem. Two distinct neural populations in the brainstem have been implicated

in respiratory rhythmogenesis: the preBötzinger Complex (preBötC), discovered in 1990 (Feldman et al., 1990; Smith et al., 1991; Feldman and Negro, 2006), and the retrotrapezoid nucleus/parafacial respiratory group (RTN/pFRG), discovered in 1989. The current hypothesis posits that these populations exist as distinct but coupled rhythm generators. In this model, the preBötC drives the rhythm, generating inspiratory movements while the RTN/pFRG is synaptically inhibited at rest, with a conditional oscillator that generates active expiration (Janczewski and Feldman, 2006; Pagliardini et al., 2011). Because of its demonstrated role in driving the respiratory rhythm, we limit our scope to the preBötC.

The preBötC is an advantageous experimental preparation because spontaneous inspiratory activity persists *in vitro* within 300-500 μm thick transverse slices containing the preBötC. Cellular activity can be recorded in the context of the network's activity, indicated by motor nerve output from the hypoglossal nerve (XIIn, **Fig. 1.1**). For many respiratory neurophysiologists, this preparation has become the basic unit of investigation. Easy access to the network by electrodes and imaging equipment has facilitated a wide range of experimental procedures that continue to provide insights into the cellular and synaptic mechanisms of respiratory rhythm generation.

Constituent neurons of the preBötC produce 300-500 ms bursts in synchrony with respiratory motor output from the XIIn (**Fig. 1.1**, Feldman and Negro, 2006). These bursts are characterized by a 10-30 mV depolarization, dubbed the inspiratory drive potential. It was hypothesized that persistent sodium current (I_{NaP}) and calcium-activated non-specific cationic current (I_{CAN}) function to augment synaptic currents to generate robust inspiratory drive potentials. Inhibition of I_{NaP} by selective antagonists (10 μM riluzole and 20 μM tetrodotoxin) did not significantly attenuate drive potential amplitude, ruling against I_{NaP} in the generation of drive potentials in the preBötC (Pace et al., 2007b). In contrast, data from Pace et al. rules in favor of I_{CAN} as a conductance underlying drive potentials.

I_{CAN} is characterized by a nonspecific monovalent cationic conductance of 25-35 pS that is activated by group I metabotropic glutamate receptors (mGluRs) (Teulon, 2000;

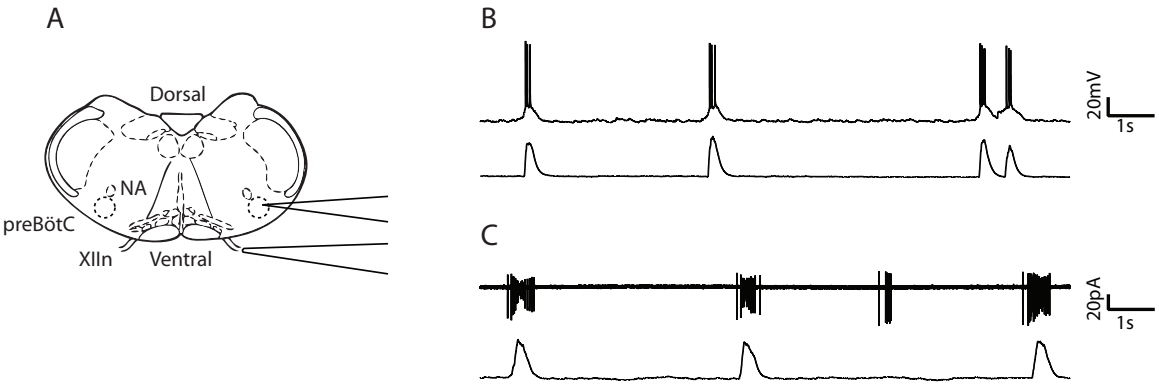

Figure 1.1: Summary diagram of experimental setup. (a) Cartoon representation of *in vitro* slice preparation from neonatal mice. (b) Upper trace: representative whole cell current-clamp recording of a preBötC neuron. Lower trace: XII respiratory motor output. (c) Upper trace: representative on-cell voltage-clamp recording of a preBötC neuron. Lower trace: XII output, as in (b).

Congar et al., 1997) and inhibition by intracellular nucleotides (e.g. ATP, ADP and AMP), flufanemic acid (FFA) and buffering of intracellular Ca^{2+} with the Ca^{2+} chelator, BAPTA (Pena and Ordaz, 2008). Pace et al. tested inspiratory drive potentials for dependence on mGluRs using selective inhibitors of group I and group II mGluRs (LY367385 and APICA, respectively). Group I, but not group II mGluRs were implicated in drive potential generation by an 1,4,5-trisphosphate (IP_3) dependent mechanism. Additionally, these investigators found that inspiratory drive potentials were attenuated by Ca^{2+} buffering by intracellular application of BAPTA and by bath application of FFA. Taken together, these data implicate I_{CAN} in the generation of inspiratory drive potentials.

While the biophysical properties of I_{CAN} are well described (Teulon, 2000), the molecular identity of this conductance remains unknown. However, the discovery of functionally unique channels within the *transient receptor potential* (TRP) family of ion channels, i.e. TRPM4/5, has provided reasonable candidates. Before discussing the structural, biophysical, and regulatory properties of TRPM4/5, it is helpful to put these family members in the context of the greater TRP superfamily.

1.2 The TRP Family of Ion Channels

Members of the transient receptor potential (TRP) superfamily, first described in *Drosophila melanogaster* visual transduction (Lo and Pak, 1981), are integral membrane proteins characterized by six transmembrane segments (S1 to S6) and a pore between S5 and S6 (Owsianik et al., 2006; Nilius and Owsianik, 2011) that functions as an ion channel. The twenty-nine TRP genes break down into seven subfamilies according to sequence homology: classic or canonical (TRPC), vanilloid (TRPV), melastatin or long (TRPM), mucolipin (TRPML), polycystin (TRPPs), and 'NO-mechano-potential C' TRPN) (Clapham et al., 2005; Nilius and Owsianik, 2011). In mammals, TRP channels are are found in a variety of tissues and cell types and have been implicated in several pathologies, including diseases of the kidney and heart, neurodegenerative disorders, and several homeostatic imbalances (for review: see Nilius and Owsianik, 2011). Within and across subfamilies, TRP channels have diverse functions, ion-permeabilities, and mechanisms of activation. This review will focus on TRPs of the TRPC and TRPM subfamilies, as previous work has demonstrated expression of these genes in preBötC cells (Crowder et al., 2007; Ben-Mabrouk and Tryba, 2010).

1.2.1 Canonical TRPs

Of all the TRP subfamilies, the seven homologs of the TRPC subfamily (TRPC1-7) share the greatest amino acid identity with the *Drosophila* TRP channels, giving the TRPCs their name. Many homologs within this subfamily are characterized by phospholipase-C-dependent (PLC) mechanisms of activation (steps 1-4, Fig. 1.3; Venkatachalam and Montell, 2007). These homologs can be subcategorized into three groups based on amino acid similarity: TRPC2, TRPC3/6/7, and TRPC1/4/5 (Nilius and Owsianik, 2011). [1] Each TRPC subfamily member is capabable of homotetramerization and, in some cases, inter-

[1] In the literature, the nomenclature of TRPC subfamilies and TRPC heteromultimers is ambiguous. Within this work, forward slashes (e.g. TRPC3/6/7) will be used to denote groups of TRP family members

and intrasubfamilial heterotetramerization, generating an enormous functional diversity (Cheng et al., 2010; Strübing et al., 2001, 2003).

TRPCs function primarily in store-operated calcium entry (SOCE) and receptor-operated Ca^{2+} entry (ROCE) (Birnbaumer, 2009). In SOCE, depletion of intracellular Ca^{2+} stores invokes an inward Ca^{2+} current independent of PLC-pathways. TRPCs have been implicated in SOCE, but the mechanism of their activation remains unknown. In ROCE, PLC activation triggers Ca^{2+} entry by activation of IP_3Rs. Notably, TRPCs are not Ca^{2+}-selective; many TRPC channels conduct monovalent cations in addition to Ca^{2+}. To date, no Ca^{2+}-impermeable TRPCs have been described, making them unlikely candidates for the monovalent I_{CAN} described by Teulon, 2000. However, heteromeric TRPCs have been found to exhibit unique biophysical properties (Strübing et al., 2001, 2003). The discovery of novel TRPC heteromers may uncover monovalent-selective TRPCs.

1.2.2 Melastatin TRPs

Proteins of the melastatin transient receptor potential subfamily (TRPMs) fall into four groups based on amino acid squence similarity: TRPM1/3, TRPM4/5, TRPM6/7, TRPM2 and TRPM8. Like other TRPs, the function and mechanism of activation varies greatly within the TRPM subfamily. TRPM1 has been implicated to function in retinal ON bipolar response pathway as a constitutively active nonspecific cationic channel (Koike et al., 2010). Additionally, though not well understood, TRPM1 mRNA expression is inversely correlated with the progression of melanomas (Prevarskaya et al., 2007). TRPM6/7 and TRPM2 are unique for their enzymatic activity. TRPM6 and TRPM7 possess an α-kinase domain used in channel regulation, and TRPM2 has a domain that functions as an ADP-ribose pyrophosphatase (Nilius and Owsianik, 2011). Most germaine to this work, however, are the unique instrinsic properties of the TRPM4/5 channels.

Structurally and functionally, the TRPM4/5 family members are very similar. TRPM4/5 are 1,214 amino-acid and 1,165 amino-acid proteins, respectively, each with a six trans-

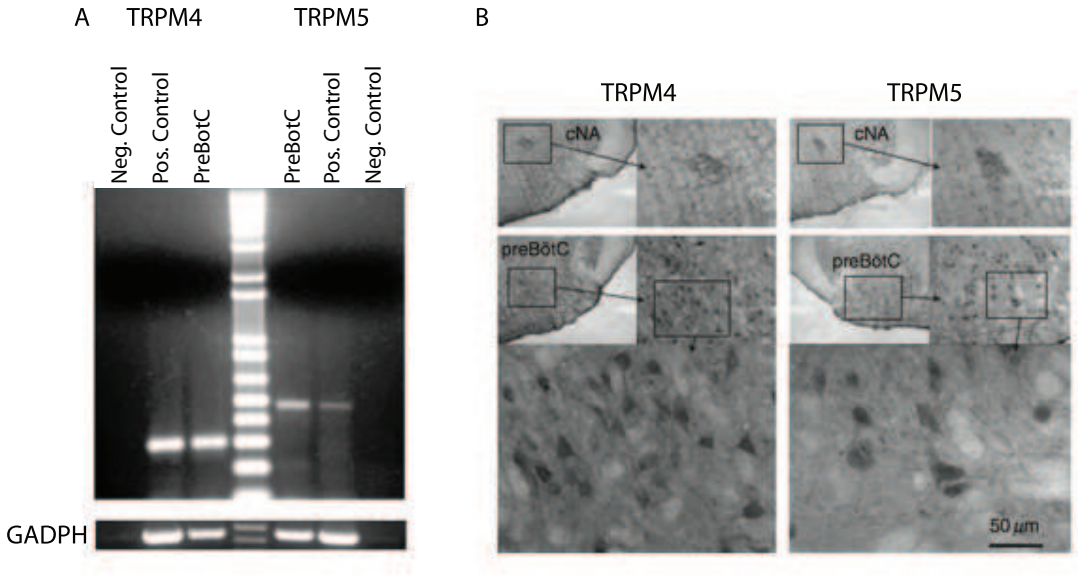

Figure 1.2: Expression of TRPM4 and TRPM5 in the preBötC. (A) Total RNA was extracted from bilateral dissections of the preBötC and murine kidney tissue expressing TRPM4 and TRPM5 (positive control), then reverse transcribed. Negative control reactions were performed without reverse transcriptase and amplified nothing. GADPH, a ubiquitously expressed gene, was used to assess quality and presence of cDNA. (B) Immunohistochemistry from adult rats. (Top panels) Dense TRPM4 and TRPM5 labeling in the region of the compac nucleus ambiguus (cNA), a known anatomical landmark of the preBötC. (Lower panels) TRPM4 and TRPM5 staining in the preBötC. (Data in (A) are reproduced with author permission from Crowder et al., 2007)

membrane domains and a pore domain between S5 and S6. These proteins share 40% amino-acid sequence homology with each other and far less homology with all other TRPs. Both channels are activated by PLC-dependent increases in intracellular Ca^{2+} ($[Ca^{2+}]_i$) (Guinamard et al., 2011). These proteins are highly sensitive to Ca^{2+}; TRPM4/5 have single-channel half-maximal effective concentrations of activation of 170 μM and 28 μM, respectively. Despite their Ca^{2+}-sensitivity, TRPM4/5 are uniquely impermeable to Ca^{2+} (Launay et al., 2002; Prawitt et al., 2003; Hofmann et al., 2003). These channels poorly differentiate between the monovalent cations Na^{+} and K^{+}. Neither channel is strictly voltage-gated because of their dependence on internal Ca^{2+} for activation; however, either channel's open probability increases with depolarization. Finally, TRPM4/5 are both regulated by PIP_2, a phospholipid component of cell-membranes. In excised patch recording, PIP_2

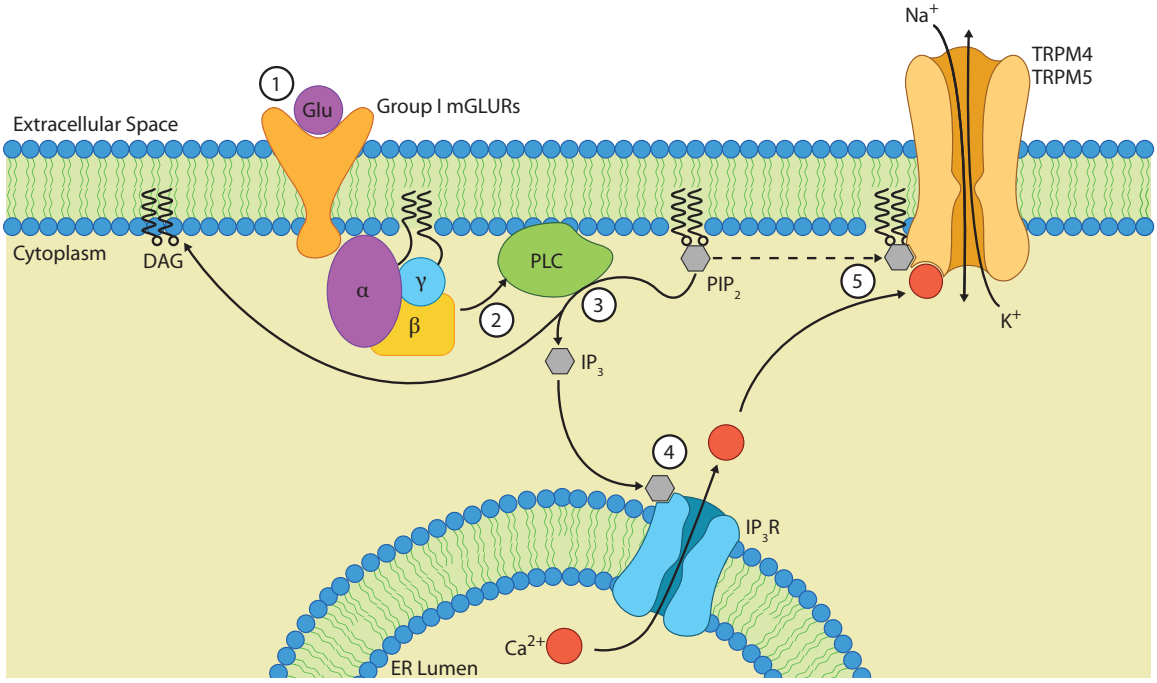

Figure 1.3: Hypothesized model of PLC-dependent I_{CAN} activation via allosteric modulation of TRPM4 or TRPM5 (1) Glutamate (Glu) binds metabotropic glutamate receptors (mGluRs), activating the heterotrimeric G protein (α, β, γ) which (2) activates phospholipase C (PLC). (3) PLC hydrolyzes phosphatidylinositol 4,5-bisphosphate (PIP_2) into 1,4,5-trisphosphate (IP_3) and diacylglycerol (DAG). (4) IP_3 binds to IP_3 receptors, releasingCa^{2+} from the lumen of the endoplasmic reticulum. (5) We propose that increased intracellular [Ca^2] gates TRPM4 and/or TRPM5 channels. Na^+ influx and K^+ efflux create a nonspecific monovalent cationic current (I_{CAN}) that generates inspiratory drive potentials. (dotted arrow) In the hypothesized model, PIP_2 directly modulates the Ca^{2+} sensitivity of TRPM4/5. (Adapted with author permission from Crowder et al., 2007).

has been shown to increase Ca^{2+}-sensitivity 100-fold.

1.2.3 Current Anatomical Evidence for TRPM4/5 Expression

Earlier RT-PCR experiments by Crowder et al., 2007 demonstrated that both TRPM4/5 are expressed in the preBötC (Fig. 1.2A). We sough to visualize TRPM4 and TRPM5 expression in the preBötC using known anatomical markers. Immunohistochemistry was performed by our colleague, Ryoichi Teruyama, on adult rats using commercial polyclonal antibodies (complete methods detailed in Appendix A). Slices taken just rostrally to the preBötC show dense TRPM4 and TRPM5 labeling in the region of the compact nucleus

ambiguus (cNA, **Fig. 1.2B**, top panels). The cNA, located immediately rostral to the preBötC, is a known anatomical landmark (Smith et al., 1991; Ruangkittisakul et al., 2006). Slices taken more caudally reveal TRPM4 and TRPM5 staining in the preBötC (**Fig. 1.2B**, lower panels).

Taken together, anatomical evidence and the established biophysical properties of these channels make them attractive candidates for I_{CAN} as described by Teulon, 2000. For these reasons, we hypothesize that TRPM4 and TRPM5 are respsonsible, at least in part, for the generation of I_{CAN} underlying robust inspiratory bursts in consituent neurons of the preBötC (Fig. 1.3).

Chapter 2

Methods

2.1 Slice Preparation

We used neonatal (postnatal day 1-5) C57 Black 6 (C57BL/6) mice in all *in vitro* electrophysiology experiments. Adult C57BL/6 mice were obtained from Harlan Sprague Daley (Indianapolis, IN, USA) and bred in-house. The Institutional Animal Care and Use Committee (The College of William and Mary) approved all protocols. Neonatal mice were anaesthetized by hypothermia (0°)C and rapidly decerebrated prior to dissection of the neuraxis in normal artificial cerebrospinal fluid (ACSF) containing (in mM): 124 NaCl, 3KCl, 1.5 $CaCl_2$, 1 $MgSO_4$, 25 $NaHCO_3$, 0.5 NaH_2PO_4, and 30 D-glucose, equilibrated with 95% O_2 and 5% CO_2, pH 7.4. Preparations were fixed to an agar wedge (containing 5% agar powder by mass in deionized H_2O) using ethyl cyanoacrylate (Krazy Glue®) and loaded rostral-surface-up into a Thermo-Scientific HM 650V vibrating microtome (Waltham, MA, USA). We cut 550μm-thick transverse slices capturing the rostral-most hypoglossal (XII) cranial nerve roots, the dorsomedial cell column, and the principal lateral loop of the inferior olivary nucleus, placing the preBötC near the rostral surface (Ruangkittisakul et al., 2006). The caudal cut captured the obex.

Slices were perfused with 26° ACSF at 4mL·min^{-1} in a 0.5mL chamber mounted

rostral-surface-up in a fixed-stage microscope. Infared-enhanced differential interference contrast (IR-DIC) videomicroscopy (Inoue and Spring, 1997) was performed using a Hitachi KP-Series charge-coupled device video camera (USA contact: Schaumburg, Illinois, USA) paired to a junction box and output to a television monitor (video in).

2.2 Electrophysiology

The ACSF K^+ concentration was raised to 9mM and respiratory motor output was recorded from XII nerve roots using suction electrodes and a differential amplifier. XII discharge was full-wave rectified and smoothed for display.

All electrical recordings were performed on inspiratory preBötC neurons selected visually by IR-DIC videomicroscopy in the region ventral to the semicompact division of the nucleus ambiguous (Gray et al., 1999; Wang et al., 2001; Ruangkittisakul et al., 2006). Cellular activity in synchrony with XII discharge confirmed inspiratory preBötC neurons. Recordings from expiratory neurons were discarded and no attempt was made to identify neurons with pacemaker properties, as these cells are not thought to be rhythmogenic (Brockhaus and Ballanyi, 1998).

Whole-cell current-clamp recordings were performed using a Dagan IX2-700 amplifier (Minneapolis, MN, USA). Data were acquired digitally at 4-20kHz using a 16-bit analog-to-digital converter (Powerlab by ADInstruments, Colorado Springs, CO, USA) after low-pass filtering at 1 kHz to avoid aliasing. Intracellular pipetttes were fabricated from capillary glass (outer diameter, 1.5mm; inner diameter, 0.87mm) using a Flaming/Brown micropipette puller (Sutter Instrument, Novato, CA, USA) and filled with standard potassium gluconate (K-gluc) solution containing (in mM): 140 potassium gluconate, 5 NaCl, 1 ethylene glycol tetraacetic acid, 10 4-(2-hydroxyethyl)-1-piperazineethanesulfonic acid (HEPES), 2 Mg-ATP, and 0.3 Na-GTP, pH 7.3 with KOH. Pipette resistance was 3-4MΩ and the liquid junction potential of K-gluc patch solution (8 mV) was corrected offline

We bath-applied 100μM 9-hydroxyphenanthrene (9-phenanthrol) dissolved in dimethylsulfoxide (DMSO) to a maximal final DMSO concentration of 0.1%; reported in Grand et al., 2008 to not affect channel activity. Baseline membrane potential was continuously monitored and maintained at -60mV with bias current to provide a consistent standard for comparing inspiratory drive potentials among preBötC neurons. Inspiratory bursts were digitally smoothed using a boxcar filter to remove spikes and the underlying inspiratory drive potentials were measured using LabChart v6.1 (ADInstruments). Labchart's Peak Parameters extension was used to measure inspiratory drive potential amplitude, half-width, and area.

On-cell and excised-patch voltage clamp recordings were performed using an Axon Instruments Axopatch-1C amplifier (Sunnyvale, CA, USA). Data acquisition was as above. Patch pipettes had a resistance of 10MΩ and were filled with patch solution containing (in mM): 149 NaCl, 3 KCl, 10 HEPES, 30 D-Glucose, 1.5 $CaCl_2 \bullet 2H_2O$, 1 $MgCl_2 \bullet 6H_2O$, and 0.5 NaH_2PO_4, pH 7.3 with KOH. After confirming inspiratory activity in the on-cell configuration, we bath-applied a modified ACSF (0 Ca^{2+} ACSF) containing (in mM): 124 NaCl, 3KCl, 30 D-Glucose, 25 $NaHCO_3$, 0.5 NaH_2PO_4, and 1 $MgCl_2$, pH 7.4 to remove on-cell inspiratory activity. Patches were excised into 0 Ca^{2+} ACSF and single-channel recordings were made. To this inside-out configuration we bath-applied 0Ca^{2+} ACSF with the Ca^{2+} concentration raised to 200μM.

Two-tailed *t*-tests were used to assess changes in inspiratory drive potential magnitude (amplitude and area). Minimum significance was set at $P < 0.05$ or less.

Chapter 3

Results

3.1 Patch-Clamp Recordings from preBötC Cells

We sought to determine the classical electrophysiological properties (voltage-dependence, linear single-channel current-voltage (I-V) relationship, and slope conducance) of preBötC neurons. However, limitations in our experimental procedure (discussed fully in Chapter 4.1) prevented the acquisition of meaningful excised-patch data. In the proposed protocol, inspiratory preBötC neurons were recorded in the on-cell configuration in 0Ca^{2+} ACSF before excision into the inside-out configuration. To assay for ion-channels activated by increases in $[Ca^{2+}]_i$, inside-out patches would be recorded in 0 Ca $^{2+}$ ACSF before being exposed to ACSF containing 200 μM Ca^{2+}. Ramp protocols (-80 mV to +80 mV) would be used to determine I-V relationship. In every attempt in which a gigaseal was obtained (n = 78 of 78; **Table 3.1**), the protocol failed to run to completion. In n = 35 attempts, patches could not be maintained in the inside-out configuration for more than 2 minutes; an insufficient amount of time for acquisition of control measurements and steady-state application of 200 μM Ca^{2+} ACSF. n = 21 patches went whole cell before 0 Ca^{2+} ACSF could be applied. In n = 22 attempts, the patch deteriorated before excision could be attempted. Analysis of on-cell channel openings from preBötC neurons recorded before excision re-

Table 3.1: Outcomes of attempted single-channel experiments

Count (n=)	Outcome
21	Patch went whole cell before 0 Ca^{2+} ACSF could be applied
35	Lost patch after excision and before protocol could be completed
22	Patch was lost before excision

vealed a conductance in the range of 25-45 pS with an average conductance of 32.8 pS (Std. Dev. = 6.3; n = 101 channel openings from 7 confirmed inspiratory patches). However, these data are preliminary in nature and must be interpreted cautiously. They can offer no insights to intracellular calcium-dependence, voltage-dependence, or pharmacological modulation.

3.2 Pharmacological Block of TRPM4

To assess a functional role for TRPM4 ion channels in generating inspiratory drive potentials, we exposed rhythmically active slice preparations to 9-phenanthrol, a selective inhibitor of TRPM4 ion channels (Grand et al., 2008), while recording XII output and membrane potential of preBötC after whole-cell dialysis with K-Gluc patch solution. Bias current was adjusted to maintain a constant baseline (V_m= -60mV). 100 μM 9-phenanthrol caused a graded attenuation of inspiratory drive potentials (Fig. 3.1A-C). No significant changes in amplitude or area were observed until after 40 and 30 minutes of 9-phenanthrol application, respectively (Fig. 3.1D). After 40 minutes of application, both amplitude and area were significantly attenuated to 21.6$\pm$0.4% and 7.6$\pm$3.5% of control, respectively (Fig. 3.1D, $P < 0.05$, n = 2). Washout with normal 9 mM K^+ ACSF for 30 minutes was unable to restore network or cellular activity. These data suggest that TRPM4 may have a functional role in the generation of inspiratory drive potentials.

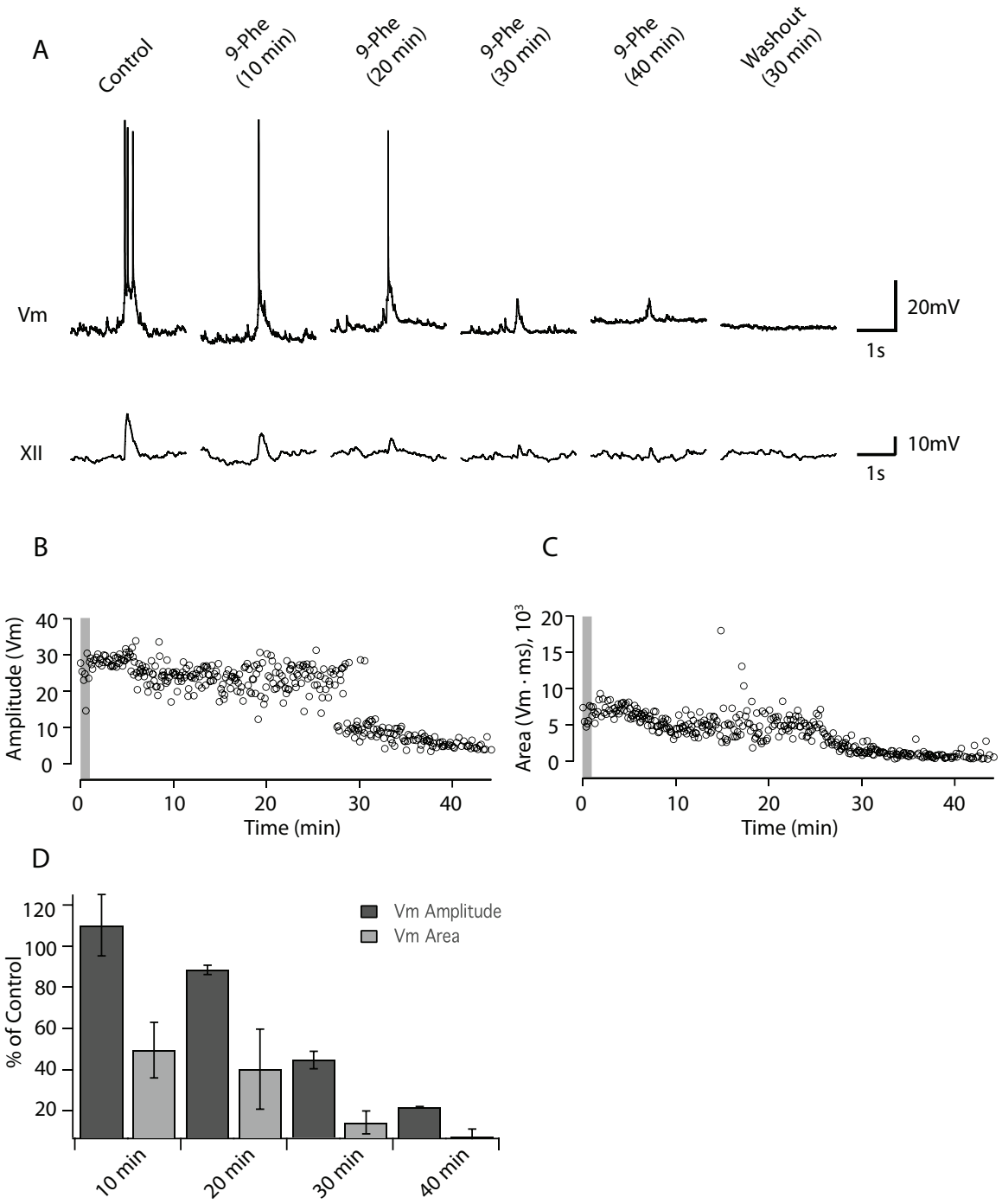

Figure 3.1: Inhibition of TRPM4 by 9-Phenanthrol. (A) 100μM 9-Phenanthrol (9-Phe) caused a progessive and irreversible attenuation of inspiratory drive potential and XII motour output magnitudes (amplitude and area). (B-C) Time course of 9-Phe-induced reduction of inspiratory drive potential amplitude (B) and area (C). Open circles represent one inspiratory cycle. The minute prior to 9-Phe application is indicated by the grey bar at time 0. (D) Bar chart demonstrating 9-Phe's effect on drive potential magnitude as a function of control. Error bars report $\pm$ S.E.M., n = 2.

Chapter 4

Discussion

Fundamentally, we seek the molecular mechanisms of inspiratory drive potential generation. Here, we continue the work begun by Crowder et al., 2007, building a case for TRPM4/5 as the molecular identity of I_{CAN}. Our current hypothesis holds that these homologs amplify synaptic input within the network to generate robust inspiratory bursts via PLC-dependent increases in $[Ca^{2+}]_i$.

4.1 Caveats and Limitations

4.1.1 Single-Channel Recordings

Our experimental preparation confers a unique and advantageous ability to study the cellular and synaptic mechanisms of respiration in the context of a functional network. For this reason, we attempted excised patch experiments from preBötC neurons in their native tissue. Doing so allows us to make single-channel recordings from confirmed inspiratory neurons, increasing the validity of our results. However, our experimental design may have inhibited collection of single-channel data. Maintenance of network activity requires constant perfusion of oxygenated ACSF. In our current configuration, the perfusate laminarly flows at a rate of $4mL \cdot min^{-1}$ through a 0.5mL recording chamber. The resulting current

likely agitated our inside-out experiments. Excised patches, once pulled from the on-cell configuration, are sensitive to flows. Consequently, our perfusion may have been displacing our patches. Additionally, extracellular material may have precluded the acquisition of gigaohm seals essential in single-channel recordings. Under the guidance of Romain Guinamard, an expert in single-channel recordings in cardiomyocytes, we propose that this investigation adopt an experimental protocol that divorces preBötC neurons from the network, discussed below.

Cellular Isolation

Dissociation and primary culture of neurons has been a research tool for decades (Dichter, 1978; Mains and Patterson, 1973). In this approach, populations of neurons are first treated with proteolytic enzymes and collagenases then gently agitated. After filtering to remove undissociated material, the isolated cells are cultured in petri dishes lined with an adhesive matrix protein (e.g. laminin, collagen) and used within twenty-four hours for patch-clamping (as described in Guinamard et al., 2004, 2006; Guinamard, 2007). In our proposed protocol, bilateral dissections of the preBötC would be subject to enzymatic digestion, isolation, and short-term culturing. Inside-out patch-clamp experiments on preBötC cells denuded of extracellular collagens would facilitate gigaohm seal-formation before excision.

Perfusion

Dissociated cells, isolated from network activity, require less stringent bath conditions. The rate of perfusion can be dramatically reduced in these preparations. We aim to redesign our perfusion mechanics, such that the perfusate accumulates in the petri dish used to fix preBötC cells. Eliminating the efflux and slowing the rate of perfusion should minimize flows and promote inside-out patch longevity. Experimental fluid exchange would be accomplished using a series of fused micropipettes, each delivering a different fluid en-

vironment (e.g. 0μM Ca^{2+}, 200μM Ca^{2+} ACSF, and a pharmacological agent). Excised patches will be exposed to experimental conditions by movement of the electrode to the immediate vacinity of the influx.

4.1.2 Pharmacology

Bath-applied pharmacology experiments must always be interpreted cautiously. It is difficult to discern whether the agent is acting on its putative target or on other factors that affect membrane excitability and synaptic drive. TRPM4, in particular, has ATP-binding cassette (ABC) signature-like motifs similar to those found in other ABC-transporters, including the cystic fibrosis transmembrane conductance regulator (CTFR, Ullrich et al., 2005) that confounds pharmacological manipulation. Additionally, TRPM4/5 are closely related homologs with similar structures. To this end, pharmacological agents that act selectively on TRPM4/5 are often unable to resolve one homolog over the other (Guinamard et al., 2011). To overcome these limitations, we used 9-phenanthrol, a pharmacological inhibitor of TRPM4 demonstrated not to affect CFTR or TRPM5 and with no other known ion channel targets (Grand et al., 2008). To date, no selective inhibitors of TRPM5 have been identified.

4.2 TRPM4 and TRPM5 are Inconclusively Implicated in Inspiratory I_{CAN}

We observed protein expression of TRPM4 and TRPM5 in the preBötC region of adult rat brainstems. This is in direct support of the work done by Crowder et al., 2007, which identified expression of TRPM4 and TRPM5 mRNA in the preBötC region of neonatal mice. Additionally, we identified a physiological role for TRPM4 in the generation of inspiratory drive potentials for the first time. However, these data are insufficient to conclude that TRPM4 and TRPM5 are the molecular identity of I_{CAN} in inspiratory neurons. Rather, this

work augments the anatomical and biophysical evidence in support of our hypothesis.

Interestingly, in *de novo* expression of either TRPM4 (TRPM4$^{-/-}$) or TRPM5 (TRPM5$^{-/-}$), there have been no reports of death due to respiratory failure (Shimizu et al., 2009; Gerzanich et al., 2009; Talavera et al., 2008, 2005; Rong et al., 2005). However, to date there have been no reports from a TRPM4/5 double-knockout (TRPM4/5$^{-/-}$). TRPM4 and TRPM5 are both expressed in the murine preBötC and their relationship with one another remains unknown. These family members may be capable of rescuing I_{CAN} by an unknown mechanism in the absence of either TRPM4 or TRPM5.

Our data is only the beginning in the investigation of TRPM4 and TRPM5's role in inspiratory drive potential generation. Much work remains to be done in the identification of inspiratory I_{CAN}'s molecular identity. No doubt the single channel protocol described here will aid in this effort. TRPM4$^{-/-}$, TRPM5$^{-/-}$, and TRPM4/5$^{-/-}$ knockout mice will also serve as potent research tools. Taken together, these techniques could answer the I_{CAN} question in the preBötC. Doing so would further our understanding of the neural control of breathing, potentially revealing viable drug targets for related pathologies.

Chapter 5

Appendices

5.1 Appendix A: Immunohistochemistry Methods

40 μm adult rat brain sections fixed with 4% paraformaldehyde were used in all immunohistochemistry experiments. Polyclonal antibodies against TRPM4 (G-20 and TRPM5 (N-20) were raised in goat against a peptide mapping at the N-terminus of human TRPM4 and TRPM5 (Santa Cruz Biotechnology, Santa Cruz, CA). Brain slicers were incubated with either TRPM4 and TRPM5 primary antibody overnight at 4°C followd by a 4-hour incubation at 21°C with biotinylated secondary antibodies (biotinylated rabbit anti-goat IgG, Vector Labs). Brain slices were incubated with avidin-biotin complex for 2 hours in accordance with the Vector Labs kit instructions. Finally, tissue was incubated for 6 minutes with diaminobenzidine (DAB) (Vector Labs) to visualize. Sections were mounted on subbed slides, allowed to air-dry overnight and cover slipped with permount.

Bibliography

Ben-Mabrouk, F. and Tryba, A. (2010). Substance p modulation of trpc3/7 channels improves respiratory rhythm regularity and ican-dependent pacemaker activity. *European Journal of Neuroscience*, 31:1219–1232.

Birnbaumer, L. (2009). The TRPC Class of Ion Channels: A Critical Review of Their Roles in Slow, Sustained Increases in Intracellular Ca2+ Concentrations*. *Annual review of pharmacology and toxicology*, 49:395–426.

Brockhaus, J. and Ballanyi, K. (1998). Synaptic inhibition in the isolated respiratory network of neonatal rats. *European Journal of Neuroscience*, 10:3823–3839.

Cheng, W., Sun, C., and Zheng, J. (2010). Heteromerization of TRP channel subunits: extending functional diversity. *Protein & Cell*, 1(9):802–810.

Clapham, D., Julius, D., Montell, C., and Schultz, G. (2005). International union of pharmacology. xlix. nomenclature and structure-function relationships of transient receptor potential channels. *Pharmacological Reviews*, 57:427–450.

Congar, P., Leinekugel, X., Ben-Ari, Y., and Crepel, V. (1997). A long-lasting calcium-activated nonselective cationic current is generated by synaptic stimulation or exogenous activation of group I metabotropic glutamate receptors in CA1 pyramidal neurons. *The Journal of neuroscience*, 17(14):5366.

Crowder, E., Saha, M., Pace, R., Zhang, H., Prestwich, G., and Negro, C. D. (2007).

Phosphatidylinositol 4,5-bisphosphate regulates inspiratory burst acvitity in the neonatal mouse preBötzinger complex. *Journal of Physiology*, 582:1047–1058.

Dichter, M. (1978). Rat cortical neurons in cell culture: culture methods, cell morphology, electrophysiology, and synapse formation. *Brain Research*, 149(2):279–293.

Feldman, J., Connelly, C., Ellenberger, H., and Smith, J. (1990). The cardiorespiratory system within the brainstem. *Eur J Neurosci*, 3:171.

Feldman, J. and Negro, C. D. (2006). Looking for inspiration: new perspectives on respiratory rhythm. *Nature Reviews Neuroscience*, 7:232–242.

Gerzanich, V., Woo, S., Vennekens, R., Tsymbalyuk, O., Ivanova, S., Ivanov, A., Geng, Z., Chen, Z., Nilius, B., Flockerzi, V., et al. (2009). De novo expression of Trpm4 initiates secondary hemorrhage in spinal cord injury. *Nature medicine*, 15(2):185.

Grand, T., Demion, M., Norez, C., Mettey, Y., Launay, P., Becq, F., Bois, P., and Guinamard, R. (2008). 9-phenanthrol inhibitis human trpm4 but not trpm5 cationic channels. *British Journal of Pharmacology*, 153:1697–1705.

Gray, P., Rekling, J., Bocchiaro, C., and Feldman, J. (1999). Modulation of respiratory frequency by peptidergic input to rhythmogenic neurons in the prebötzinger complex. *Science*, 52:1566–1568.

Guinamard, R. (2007). Determination of Channel Properties at the Unitary Level in Adult Mammalian Isolated Cardiomyocytes. *Methods in Molecular Biology*, 403:195.

Guinamard, R., Chatelier, A., Demion, M., Potreau, D., Patri, S., Rahmati, M., and Bois, P. (2004). Functional characterization of a Ca2+-activated non-selective cation channel in human atrial cardiomyocytes. *The Journal of Physiology*, 558(1):75.

Guinamard, R., Demion, M., Magaud, C., Potreau, D., and Bois, P. (2006). Functional

expression of the TRPM4 cationic current in ventricular cardiomyocytes from spontaneously hypertensive rats. *Hypertension*, 48(4):587.

Guinamard, R., Sallé, L., and Simard, C. (2011). The Non-selective Monovalent Cationic Channels TRPM4 and TRPM5. *Transient Receptor Potential Channels*, pages 147–171.

Hofmann, T., Chubanov, V., Gudermann, T., and Montell, C. (2003). TRPM5 is a voltage-modulated and Ca2+-activated monovalent selective cation channel. *Current biology*, 13(13):1153–1158.

Inoue, S. and Spring, K. (1997). *Video Microscopy: the Fundamentals*. Plenum Press.

Janczewski, W. and Feldman, J. (2006). Distinct rhythm generators for inspiration and expiration in the juvenile rat. *The Journal of Physiology*, 570(2):407–420.

Koike, C., Numata, T., Ueda, H., Mori, Y., and Furukawa, T. (2010). TRPM1: A vertebrate TRP channel responsible for retinal ON bipolar function. *Cell calcium*.

Launay, P., Fleig, A., Perraud, A., Scharenberg, A., Penner, R., and Kinet, J. (2002). TRPM4 is a Ca2+-activated nonselective cation channel mediating cell membrane depolarization. *Cell*, 109(3):397–407.

Lo, M. and Pak, W. (1981). Light-induced pigment granule migration in retinular cells of *Drosophila melanogaster*. *The Journal of General Physiology*, 77:155–175.

Mains, R. and Patterson, P. (1973). Primary cultures of dissociated sympathetic neurons. *The Journal of cell biology*, 59(2):329.

Marieb, E. (2009). *Human Anatomy & Physiology*. Pearson Eduction, Inc.

Nilius, B. and Owsianik, G. (2011). The transient receptor potential family of ion channels. *Genome Biology*, 12:218.

Owsianik, G., D'Hoedt, D., Voets, T., and Nilius, B. (2006). Structure-function relationship of the trp channel superfamily. *Reviews of Physiology, Biochemistry & Pharmacology*, 156:61–90.

Pace, R., Mackay, D., Feldman, J., and Del Negro, C. (2007a). Inspiratory bursts in the preBotzinger complex depend on a calcium-activated non-specific cation current linked to glutamate receptors in neonatal mice. *The Journal of Physiology*, 582(1):113–125.

Pace, R., Mackay, D., Feldman, J., and Del Negro, C. (2007b). Role of persistent sodium current in mouse preB

"otzinger complex neurons and respiratory rhythm generation. *The Journal of physiology*, 580(2):485–496.

Pagliardini, S., Janczewski, W., Tan, W., Dickson, C., Deisseroth, K., and Feldman, J. (2011). Active Expiration Induced by Excitation of Ventral Medulla in Adult Anesthetized Rats. *The Journal of Neuroscience*, 31(8):2895.

Pena, F. and Ordaz, B. (2008). Non-selective cation channel blockers: potential use in nervous system basic research and therapeutics. *Mini reviews in medicinal chemistry*, 8(8):812–819.

Prawitt, D., Monteilh-Zoller, M., Brixel, L., Spangenberg, C., Zabel, B., Fleig, A., and Penner, R. (2003). TRPM5 is a transient Ca2+-activated cation channel responding to rapid changes in [Ca2+] i. *Proceedings of the National Academy of Sciences of the United States of America*, 100(25):15166.

Prevarskaya, N., Zhang, L., and Barritt, G. (2007). TRP channels in cancer. *Biochimica et Biophysica Acta (BBA)-Molecular Basis of Disease*, 1772(8):937–946.

Rong, M., He, W., Yasumatsu, K., Kokrashvili, Z., Perez, C., Mosinger, B., Ninomiya, Y., Margolskee, R., and Damak, S. (2005). Signal transduction of umami taste: insights from knockout mice. *Chemical Senses*, 30(suppl 1):i33.

Ruangkittisakul, A., Schwarzacher, S., Sechhia, L., Poon, B., Ma, Y., Funk, G., and Ballayani, K. (2006). High sensitivity to neuromodulator-activated signaling pathways at physiological K^+ of confocally imaged respiratory center neurons in on-line-calibrated newborn rat brainstem slices. *Journal of Neuroscience*, 26:11870–11880.

Shimizu, T., Owsianik, G., Freichel, M., Flockerzi, V., Nilius, B., and Vennekens, R. (2009). TRPM4 regulates migration of mast cells in mice. *Cell calcium*, 45(3):226–232.

Smith, J., Ellenberger, H., Ballanyi, K., Richter, D., and Feldman, J. (1991). Pre-Botzinger complex: a brainstem region that may generate respiratory rhythm in mammals. *Science*, 254(5032):726.

Strübing, C., Krapivinsky, G., Krapivinsky, L., and Clapham, D. (2001). TRPC1 and TRPC5 form a novel cation channel in mammalian brain. *Neuron*, 29(3):645–655.

Strübing, C., Krapivinsky, G., Krapivinsky, L., and Clapham, D. (2003). Formation of novel TRPC channels by complex subunit interactions in embryonic brain. *Journal of Biological Chemistry*, 278(40):39014.

Talavera, K., Yasumatsu, K., Voets, T., Droogmans, G., Shigemura, N., Ninomiya, Y., Margolskee, R., and Nilius, B. (2005). Heat activation of TRPM5 underlies thermal sensitivity of sweet taste. *Nature*, 438(7070):1022–1025.

Talavera, K., Yasumatsu, K., Yoshida, R., Margolskee, R., Voets, T., Ninomiya, Y., and Nilius, B. (2008). The taste transduction channel TRPM5 is a locus for bitter-sweet taste interactions. *The FASEB Journal*, 22(5):1343.

Teulon, J. (2000). Ca2+-activated non-selective cation channels. *Handbook of experimental pharmacology*, 147:625–649.

Ullrich, N., Voets, T., Prenen, J., Vennekens, R., Talavera, K., Droogmans, G., and Nilius, B. (2005). Comparison of functional properties of the Ca2+-activated cation channels TRPM4 and TRPM5 from mice. *Cell Calcium*, 37(3):267–278.

Venkatachalam, K. and Montell, C. (2007). TRP channels. *Annu. Rev. Biochem.*, 76:387–417.

Wang, H., Stornetta, R., Rosin, D., and Guyenet, P. (2001). Neurokinin-1 receptor-immunoreactive neurons of the ventral respiratory group in the rat. *Journal of Computational Neuroscience*, 434:128–146.